INFLUENCE OF THE PRE-TREATMENT OF GLASS SUBSTRATES ON LASER-INDUCED BACKSIDE WET ETCHING USING NIR NANOSECOND-PULSES AND CU-BASED SOLUTIONS

Authors:

P. Schwaller, S. Zehnder, U. von Arx, B. Neuenschwander

Corresponding author: P. Schwaller

e-mail: patrick.schwaller@bfh.ch

Influence of the pre-treatment of glass substrates on Laser-Induced Backside Wet Etching using NIR Nanosecond-Pulses and Cu-based solutions

P. Schwaller[1], S. Zehnder[1], U. von Arx[2], B. Neuenschwander[1]

[1]Institute for Applied Laser, Photonics and Surface Technologies, Bern University of Applied Sciences, Pestalozzistrasse 20, CH-3400 Burgdorf
[2]Department Architecture, Wood and Civil Engineering, Bern University of Applied Sciences, Solothurnstrasse 102, CH-2500 Biel

Abstract

Laser induced backside wet etching (LIBWE) has shown to be a promising tool for the micro-structuring of transparent materials. Our group has investigated LIBWE using NIR ns-laser pulses and Cu-based absorber liquids. Focus of this paper is to investigate the influence of the pre-treatment of the transparent substrate on ablation. For this purpose experiments were done on untreated and silanized soda lime glass surfaces. Our results show that depending on the absorber liquid the silanization of the substrate either enhances or delays the ablation. Possible ablation models for the different experimental settings will be discussed.

Introduction

Laser-induced back side wet etching (LIBWE) is a promising tool for applying microstructures to transparent substrates. Application fields are for example micro-optical, micro-mechanical or micro-fluid components [1-3]. In a typical LIBWE experiment (see Figure 1) laser light is directed through a transparent material and is absorbed in a liquid at the back side of the transparent material [4].
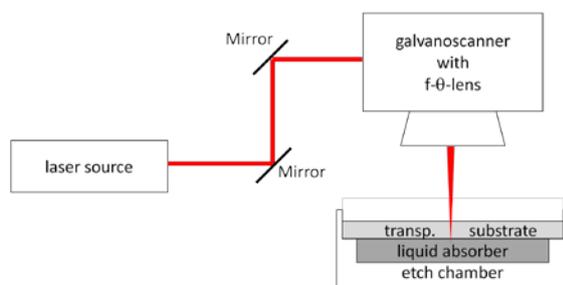
Figure 1
Schematic experimental setup for the LIBWE experiments

Depending on the used laser light and the absorbing liquid, thermal effects or shock waves lead to micro-ablation at the rear side of the glass surface. Most current applications of LIBWE use UV excimer lasers (ns pulse duration) and aromatic hydrocarbons or liquid heavy metals as absorbers [4,5]. The desired structures are achieved by irradiating through a mask [6]. In recent work [7,8] we have demonstrated that LIBWE is also working using ns laser pulses at 1064 nm wavelength and Cu-based absorber solutions. This specific LIBWE setup could be interesting especially for industrial applications because NIR-ns-laser systems are widely used and also affordable. In addition, Cu-based absorber liquids like $CuSO_4$ in aqueous solution are rather easy to handle and not hazardous (compared to liquid heavy metals for example). We have investigated the ablation mechanism for this specific setup using soda lime glass as test substrates. The soda lime substrates were used in two different modifications: Standard and cleaned substrates (see Figure 2a) are labeled in the following "untreated", soda lime substrates were large parts of the surface are saturated by CH_3-groups (see Figure 2b) will be labeled "silanized". Details about the silanization process are described in the experimental section.

As discussed in [7] it is assumed that for $CuSO_4$ in aqueous solution (also referred to as $CuSO_4$ in the following) the ablation at the surface of the transparent substrate takes place due to adsorbed Cu^{2+} species that are present in the solution (see Figure 2a). The adsorption of Cu^{2+} at the untreated surface is likely because this modification of the soda lime substrate has a polar surface. For the aqueous $CuSO_4$ solution Cu^{2+} ions are attracted by the polar glass surface due to Coulomb interaction and physisorbtion at the glass surface (see Figure 2a). This occurs without the need of a laser pulse. During the LIBWE experiment, the 1064 nm pulses are absorbed by the Cu^{2+} ions (at the glass surface and in the liquid). It is expected that for pulse lengths of around 20 ns and for copper as absorbing material the absorbed energy is transformed mostly into heat [9]. In our case heat is transferred from the Cu^{2+} ions at the glass surface to the soda lime glass. This is followed by a local (only a few atoms are

involved) micro-ablation due to thermally induced stress. The actual ablation is therefore a one-step process. Laser pulses that are absorbed by Cu^{2+} ions in the liquid transfer their energy also in form of heat to the surrounding liquid. Because the water acts as a heat sink, this has no further effect. Note in this context also that the specific heat capacity is 4.18 J/gK for H_2O at 25°C, whereas it is only about 0.8 J/gK for glass.

Our experiments (see [7] and this work) show that if the adsorption sites (or large parts of the adsorption sites) are blocked by CH_3-groups due to the silanization treatment (see Figure 2b), the ablation onset is delayed. This corroborates the ablation model described above.
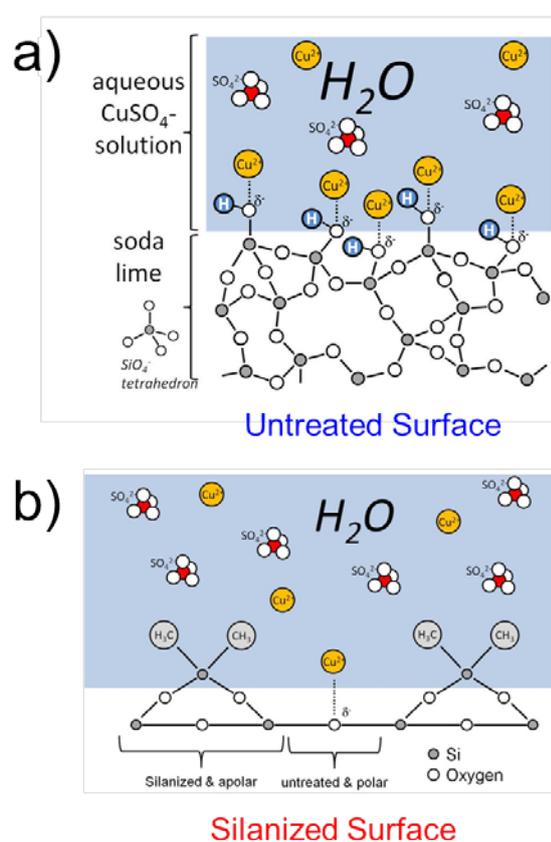
Figure 2
(a) Untreated soda lime glass surface in contact with $CuSO_4$ in aqueous solution. The Cu^{2+} ions in the solution are attracted by the polar soda lime glass surface. (b) Silanized soda lime glass surface: Most of the adsorption sites for Cu^{2+} are blocked by CH_3-groups (see text for more detailed information).

The main focus of this paper is to investigate how ablation compares between "untreated" and "silanized" substrates if a neutral species like Cu^0 is adsorbed at the substrates surface. Such a configuration can be obtained if instead of $CuSO_4$ in aqueous solution, aqueous $CuSO_4$ in form of a tartrate-complex (CuL_2) and with formaldehyde as electron donor is used as absorber liquid. Here, ablation is expected to be a two-step process. First,

electrically neutral metallic Cu species (Cu^0) are formed by a photo-induced process due to absorbed laser pulses according to equation (1).

$$[CuL_2]^{2-} + 2\ HCOH + 4\ OH \rightarrow$$
$$Cu^0 + 2L^{2-} + H_2 + 2\ H_2O + 2\ HCOO^- \qquad (1)$$
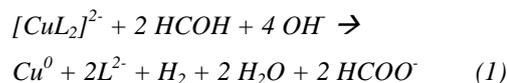
In equation (1) L is the complexing agent, which is used to prevent the precipitation of the copper hydroxide. OH^- is needed for the redox reaction of formaldehyde (HCOH) and copper, and no excess OH^- is present that could interact with the glass surface. Cu^0 formed according equation (1) is likely to agglomerate to clusters of probably several hundred to thousand atoms and these clusters subsequently adsorb on the glass surface. Note that in this case the adsorption at the surface is not driven by Coulomb interaction since the Cu^0 clusters are nonpolar. However, similar to the Cu^{2+} ablation process the actual ablation for CuL_2 is a consequence of heat transfer from the Cu^0 to the soda lime glass. The ablation process using CuL_2 as an absorber is therefore a two-step process whereas for $CuSO_4$ with Cu^{2+} as an absorber a single absorption event is responsible for the ablation.

Because the different surface polarity (between untreated and silanized soda lime substrates) should not affect the adsorption behavior of Cu^0 species, the ablation behavior is expected to be similar for the two substrate surface modification and CuL_2 as absorber liquid.

Experimental

In the following section the experimental setup used for the experiments presented in this paper as well as the surface preparation steps and the analysis tools used for the investigation of the ablated surfaces are briefly described.

Surface preparation

All results presented in this paper have been obtained using soda lime glasses as substrates. The substrates have been cleaned prior to the LIBWE experiments using the so-called RCA cleaning procedure [10] commonly used in semiconductor industry for substrate cleaning. These substrates will be labeled untreated in this paper. Some untreated substrates were in addition treated with a dimethyldichlorsilane ((CH_3)$_2SiCl_2$) solution in dry toluene. The effect of this procedure is that large parts of the soda lime glass surface are saturated by CH_3-groups (see Figure 2b). For results obtained on these surfaces the label "silanized" will be used in the following.

LIBWE setup

The LIBWE experiments were performed using a pulsed Ytterbium fiber laser of 1064 nm center

wavelength and with 20 ns pulses (YLPM series, IPG Laser GmbH). For all experiments presented in this work the pulse repetition rate has been set to 100 kHz. For this work only line structures have been ablated using a galvanoscanner equipped with a 100 mm f-Θ-lens. The resulting spot had a diameter of about 40 μm. As absorber liquids aqueous $CuSO_4$ (also referred to as $CuSO_4$ in the following) and aqueous $CuSO_4$ in form of a tartrate-complex (also referred to as CuL_2 in the following) and with formaldehyde as electron donor were used. CuL_2 is known as precursor for photo-induced metal deposition at a wavelength of 532 nm [11]. The absorbance of $CuSO_4$ was 1.7 mm^{-1}, for CuL_2 0.05 mm^{-1}. To ensure that all observed effects in the LIBWE experiments are due to the aqueous $CuSO_4$ and CuL_2 absorber liquids, control experiments have been done on untreated and silanized soda lime glass and pure H_2O as liquid. In neither of the two cases ablation effects have been observed.

Analysis of ablated structures

The topography of the ablated line structures have been qualitatively inspected by optical microscopy. The ablated structures have been investigated by using a confocal laser scanning microscope LSM (Zeiss LSM Pascal 5) and quantitative information about the average ablation rate per laser pulse could be inferred from the topographical data. Further investigations of the substrate surfaces have been done by tapping-mode atomic force microscopy AFM (Digital Instruments DI3100). In tapping mode AFM the oscillation of the AFM cantilever is modified due to interactions with the surface that is investigated [12]. These interactions modify on the one hand the amplitude of the oscillations, on the other hand also a phase shift $\Delta\Phi$ compared to the freely oscillating cantilever occurs. Whereas the amplitude signal reveals information about the topography of the measured surface, the phase shift signal contains information about the mechanical properties of the near surface zone of the measured sample [12]. The magnitude of the phase $\Delta\Phi$ is a measure of the stiffness of the near surface zone - see equation (2) – as long as the topography is not too corrugated.

$$|\Delta\Phi| \propto Stiffness \qquad (2)$$

In addition, also the sign of the phase change $\Delta\Phi$ yields information about the interaction between the sample surface and a cantilever tip in its proximity. If the phase change is negative, then the sum of the force changes due to interactions between surface and cantilever tip is attractive (see equation (3)).

$$\Delta\Phi < 0 \Rightarrow \sum_i \frac{\partial F_i}{\partial z} \ attractive \qquad (3)$$

If the phase change is positive (see equation (4)), the sum of the force changes present due to the

interaction between surface and cantilever tip is repulsive.

$$\Delta\Phi > 0 \Rightarrow \sum_i \frac{\partial F_i}{\partial z} \ repulsive \qquad (4)$$

If we assume that the AFM cantilever tip is electrically neutral then the interaction between the tip and the sample surface should not be influenced by the polarity of the sample. As a consequence the distribution of the measured phase changes should be centered around zero phase change. This is indeed what is observed in the measurement (see Figure 9 in the results section of this paper). A similar reasoning can now be made if the cantilever tip in the interaction is "replaced" by another neutral object as the Cu^0 species if the CuL_2 absorber is used in a LIBWE experiment. We therefore assume that the adsorption of Cu^0 species is similar for untreated and silanized soda lime glass surface.

Results

To study the influence of the surface modification of the substrate (untreated and silanized) for the two absorber liquids line structures were made with different numbers of iterations, i.e. different number of times the laser beam passes a specific location of the substrate surface.

Ablation behavior
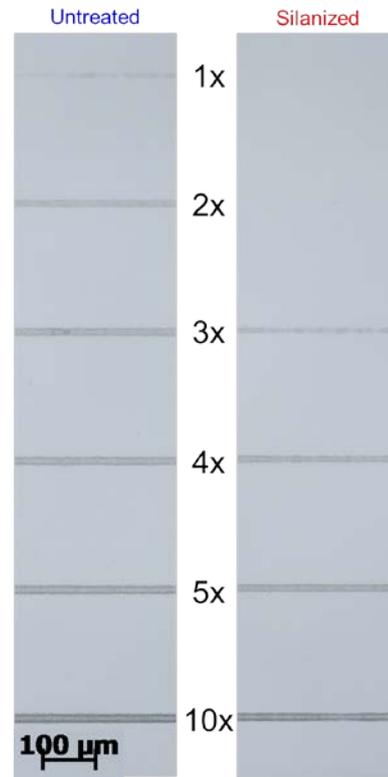
Figure 3
Optical micrographs of ablation tracks obtained with $CuSO_4$ for untreated (left) and silanized (right) soda lime glass. Ablation tracks for different number of passes are shown.

Figure 3 shows optical micrographs of ablation tracks obtained with $CuSO_4$ as absorber for untreated (left part of Figure 3) and silanized (right part of Figure 3) soda lime glass surfaces for different number of passes. The used fluence was 5 J/cm^2 and the scanning velocity was set to 20 mm/sec.

It can be clearly seen from Figure 3 that the onset of ablation is delayed for the silanized surface. The same conclusion can also be drawn from the average ablation rate values shown in Figure 4.
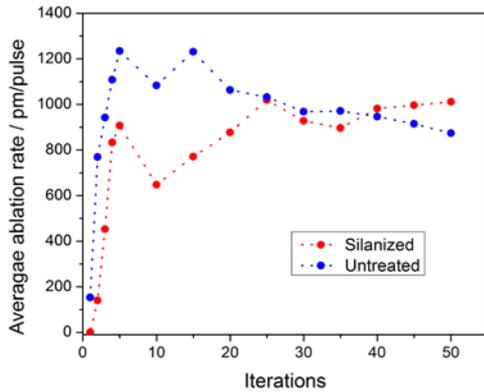
Figure 4
Average ablation rates as a function of the number of passes obtained with $CuSO_4$ as absorber for untreated (blue) and silanized (red) soda lime glass surfaces. The dashed lines serve as guide to eye.

In agreement with the observations that can be made from the optical micrographs, also the average ablation rates reveal the delayed ablation onset for the silanized surface. This can be inferred from the slight shift of the red curve (silanized surface) towards higher iteration numbers compared to the blue curve which represents the average ablation rates for the untreated surface. In addition the average ablation rate for the silanized surface are lower for low iteration numbers because the number of adsorption sites for Cu^{2+} is reduced due to the silanization. As discussed in the introductory chapter and in [7], this behavior is consistent with a partial blocking of the Cu^{2+} absorption sites by the CH_3-groups on the silanized surface. Once all silanized sites with the CH_3-groups are removed the average ablation rate values for the silanized surface reach the values as measured from the untreated surface. Figure 5 shows optical micrographs of ablation tracks obtained with CuL_2 as absorber liquid for untreated (left part of Figure 5) and silanized (right part of Figure 5) soda lime glass substrates for different number of passes. Here the fluence was 7 J/cm^2 and the scanning velocity was set to 1 mm/sec. In contrast to what was expected for the LIBWE process using CuL_2 as absorber liquid, we observe clear differences of the ablation behavior between untreated and silanized surfaces. Here, however, the ablation for the

silanized surface is enhanced for low iteration numbers compared to the untreated surface. Again this is also confirmed by the average ablation rate values shown in Figure 6. The average ablation rates for the silanized surface are almost four-times higher at the beginning of the ablation process and the reach the lower values that are measured for the untreated surface. Because these findings are not explained by our ablation model as presented in the introduction, we conducted tapping-mode AFM measurements on untreated and silanized surfaces to investigate the local topography and mechanical properties of the two surface modifications. Results are presented in the next section.
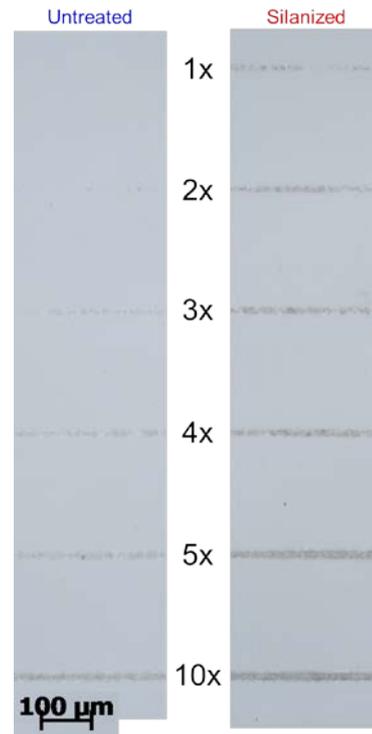
Figure 5
Optical micrographs of ablation tracks obtained with CuL_2 for untreated (left) and silanized (right) soda lime glass. Ablation tracks for different number of passes are shown.
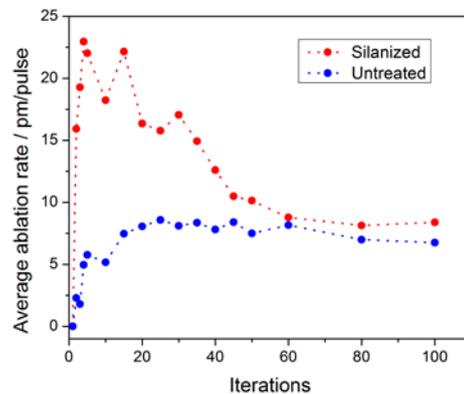
Figure 6
Average ablation rates as a function of the number of passes obtained with CuL_2 as absorber for untreated (blue) and silanized (red) soda lime glass surfaces. The dashed lines serve as guide to eye.

AFM investigations

Figure 7 shows a 1 µm x 1 µm AFM topography scan of an untreated (upper image of Figure 7) and a silanized (lower image of Figure 7) soda lime surface before the LIBWE experiments. Note again that the topography image is a measure of the amplitude variation of the oscillating AFM cantilever.

TOPOGRAPHY

Untreated
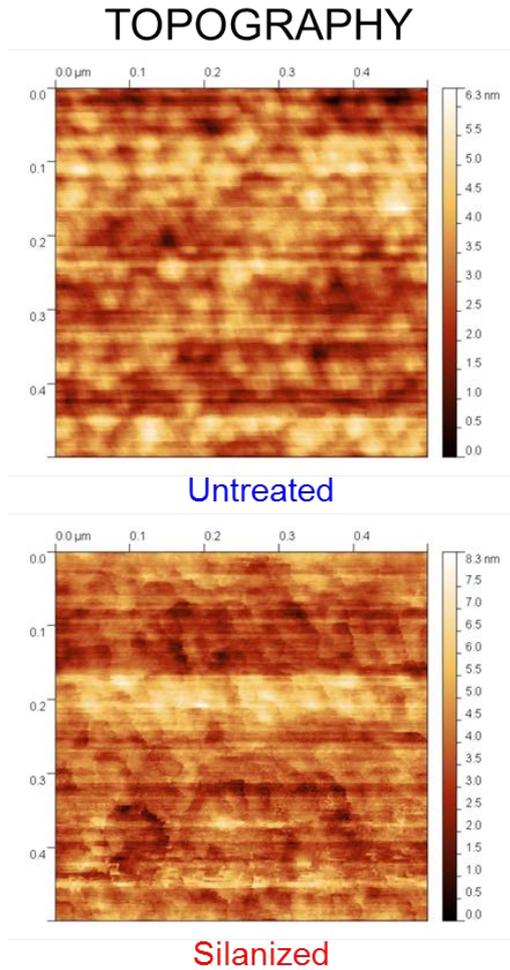
Silanized

Figure 7
Local topography for an untreated and a silanized soda lime glass surface as measured by AFM.

As can be seen the topography of the two surface modifications is not very different. This has also been confirmed by analyzing the R_a roughness values from several different measurements. The result is shown in Table 1.

Table 1: R_a roughness values for untreated and silanized soda lime glass substrates. The values in brackets indicate the standard deviation from several measurements

Substrate	R_a / nm
Untreated	1.0 (0.2)
Silanized	0.9 (0.2)

Looking at the corresponding phase image (i.e. the phase change $\Delta\Phi$ of the oscillating cantilever due to interaction with the surface) of the topography images shown in Figure 7 however, clear differences can be observed. The phase images of an untreated (upper image) and a silaized surface (lower image) are shown in Figure 8.

PHASE IMAGE

Untreated
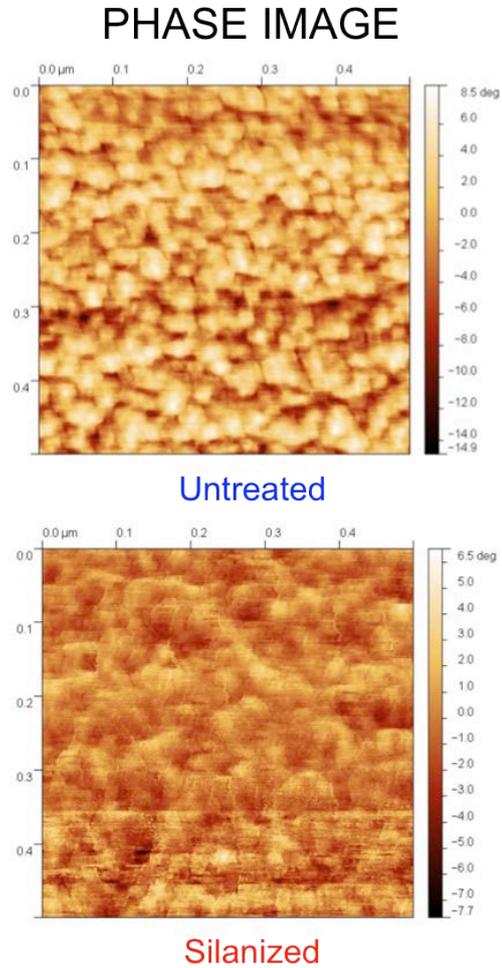
Silanized

Figure 8
Local mapping of the phase change signal for an untreated and a silanized soda lime glass surface as measured by AFM.

The phase image shows a more pronounced phase variation for the untreated surface compared to the silanized surface. The effect gets even more evident if the distribution of the phase change $\Delta\Phi$ is plotted (see Figure 9).

From Figure 9 it can be seen that both distributions are centered around zero phase change. According to equations (3) and (4) this is an indication that the adsorption probability of the Cu^0 species is similar for both types of surfaces. The magnitude of the phase change $|\Delta\Phi|$ however is much larger for the untreated surface compared to the silanized surface. According to equation (2) this would indicate that the near surface zone of the untreated substrate is stiffer than the near surface zone of the

silanized surface. Within the context here near surface zone means roughly a depth of 1-2 nm from the surface.
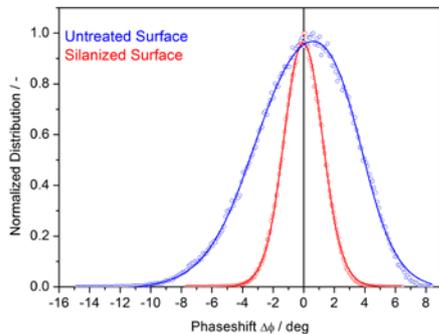
Figure 9
Distribution of the phase change (obtained from the same data sets as used for the images in Figure 8) for an untreated (blue) and silanized (red) soda lime glass surface. The solid lines serve as guide to the eye.

As can be inferred from the Figures 5 and 6 the ablation process using CuL_2 and silanized surfaces as substrates proceeds in a similar way as the process on untreated substrates after several passes of the laser beam. To investigate this kind of "transition" from the silanized surface to the untreated surface we determined the phase distribution curves for different numbers of passes of the laser beam. The result for the untreated surface can be seen in Figure 10. The phase distribution curve for the first iteration is colored in black for better visibility.
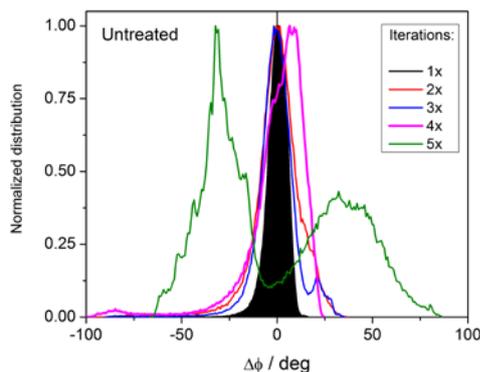
Figure 10
Evolution of the phase change distribution with the number of passes for an untreated soda lime substrate and CuL_2 as absorber liquid.

From Figure 10 it can be seen that for the first three iterations the distribution is more or less centered around zero phase change, the only difference is a broadening of the distribution. The distribution of the fourth iteration still has a component around $\Delta\Phi=0$ but also shows a second component with

$\Delta\Phi>0$. The phase distribution for the fifth iteration shows a completely different behavior. As it can be seen from Figure 5, after five iterations a clear ablation track is visible. As a consequence the phase signal of the AFM measurement is somehow convoluted with topographical information and does therefore not only contains information about the mechanical properties of the near surface zone. In all measurements we observed such an "erratic" behavior of the phase distribution as soon as a clearly visible ablation topography is present.

Similar measurements but now for the silanized surface and CuL_2 as absorber liquid are shown in Figure 11. The phase distribution for the first iteration is very narrow and is again colored in black for better visibility.
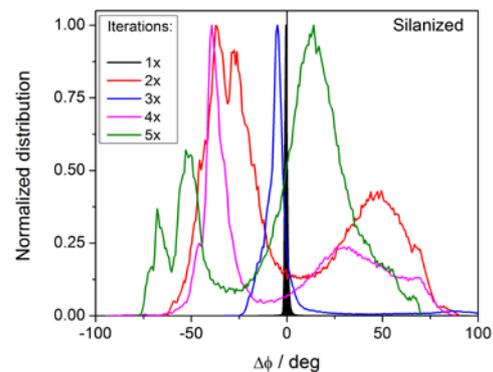
Figure 11
Evolution of the phase change distribution with the number of passes for a silanized soda lime substrate and CuL_2 as absorber liquid.

It can be seen that in this case only for the first iteration a nicely shaped distribution around zero phase change is observed, already from the second iteration the "erratic" behavior typical for ablation is observed. This again is consistent with the optical micrographs shown in Figure 5.

The consequences of these findings for the proposed ablation mechanisms are discussed in the next section.

Discussion

The results presented in the previous sections indicate that for $CuSO_4$ as absorbing liquid an ablation process based on adsorbed Cu^{2+} ions at the substrate surface is likely. The experiments on the silanized surfaces where the onset of ablation was found to be delayed are consistent with our assumption. The reason of the differences can be explained by the different ability of Cu^{2+} ions to adsorb at untreated and silanized soda lime glass surfaces due to their different polarities. For the CuL_2 absorber with the neutral Cu^0 species a

different surface polarity does not explain the observed differences in ablation (see Figures 5 and 6). The phase information obtained from AFM measurements however gives indications that the mechanical properties of untreated and silanized soda lime surfaces within a depth of the first few nanometers from the surface is different. A higher stiffness of the untreated substrate – as indicated by the phase information – is indeed consistent with the observed ablation properties. Note that this difference of the substrate stiffness is also present for $CuSO_4$ as absorber liquid. However, here the differences in ablation are ruled by the different adsorption properties of Cu^{2+} ions and not by the stiffness differences.

Summary

The LIBWE experiments performed on untreated and silanized soda lime glass substrates with two different absorber liquids show that even faint substrate modifications like attached CH_3-groups can significantly modify the ablation behavior. It is assumed that the CH_3-groups alter the stiffness of the surface region. It is planned to corroborate this assumption by nanoindentation (yielding hardness and elastic modulus) measurements of the surface zone. In any case the results show that for a high reproducibility using the LIBWE process with ns-laser pulses in the NIR regime and Cu-based absorber solutions, special attention should be drawn to a proper cleaning and handling of the substrates.

Acknowledgements

References

[1] K. Zimmer and R. Böhme (2005), Precise etching of fused silica for refractive and diffractive micro-optical applications, Optics and Lasers in Engineering 43, 1349–1360

[2] B. Hannes et al. (2008), The etching of glass patterned by microcontact printing with application to microfluidics and electrophoresis, Sensors and Actuators B 129, 255–262

[3] J. M. Fernandez-Pradas, D. Serrano, P. Serra and J. L. Morenza (2009), Laser fabricated microchannels inside photostructurable glass-ceramic, Applied Surface Science 255, 5499–5502

[4] J. Wang, H. Niino and A. Yabe (1999), Micromachining of quartz crystal with excimer lasers by laser-induced backside wet etching, Appl. Phys. A 69, 271–S273

[5] K. Zimmer, R. Böhme, D. Hirsch and B. Rauschenbach (2006), Backside etching of fused silica with UV laser pulses using mercury, J. Phys. D: Appl. Phys. 39, 4651–4655

[6] Z. Q. Huang, M. H. Hong, T. B. M. Do and Q. Y. Lin (2008), Laser etching of glass substrates by 1064 nm laser irradiation, Appl Phys, 159–163

[7] P. Schwaller, S. Zehnder, U. von Arx and B. Neuenschwander (2011). A novel Model for the Mechanism of Laser-Induced Back Side Wet Etching in Aqueous Cu Solutions using ns Pulses at 1064 nm, Physics Procedia, Volume 12, Part B, 188-194

[8] S. Zehnder, P. Schwaller, U. von Arx, G. Bucher and B. Neuenschwander (2011), Micro structuring of transparent materials with NIR ns-laser pulses, Physics Procedia, Volume 12, Part B, 195-200

[9] B. N. Chichkov, C. Momma, S. Nolte, F. von Alvensleben and A. Tünnermann (1996) Femtosecond, picosecond and nanosecond laser ablation of solids, Appl. Phys. A 63, 109-115

[10] W. Kern and D. A. Puotinen (1970), Cleaning solutions based on hydrogen peroxide for use in silicon semiconductor technology, RCA Rev. 31, 187-206

[11] A. Manshina et al. (2007), Laser-assisted metal deposition from $CuSO_4$-based electrolyte solution, Laser Phys. Lett. 4, 163-167

[12] See for example: Handbuch der Nanoanalytik (2005), W. Rom, Editor, Nanonet Styria